

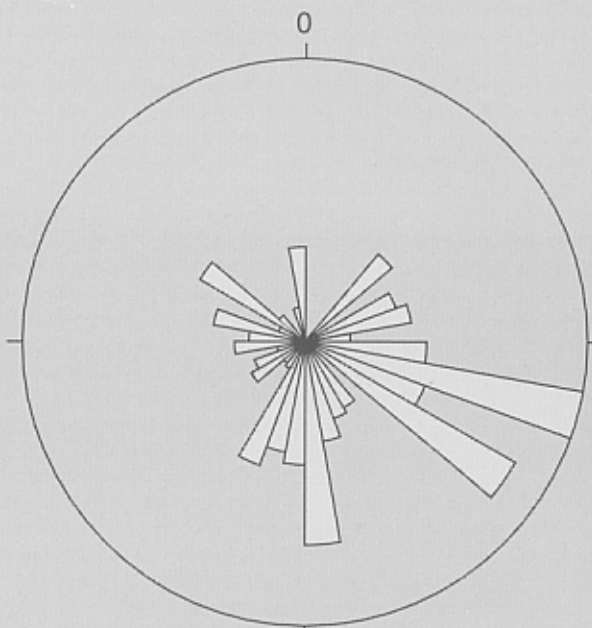
Prepared in cooperation with the
U.S. ENVIRONMENTAL PROTECTION AGENCY, REGION 1

Characteristics of Fractures in Crystalline Bedrock Determined by Surface and Borehole Geophysical Surveys, Eastern Surplus Superfund Site, Meddybemps, Maine

Water-Resources Investigations Report 99-4050



Lower-hemisphere stereonet
contour plot



Rose diagram showing
dip direction

U.S. Department of the Interior
U.S. Geological Survey

Characteristics of Fractures in Crystalline Bedrock Determined by Surface and Borehole Geophysical Surveys, Eastern Surplus Superfund Site, Meddybemps, Maine

By BRUCE P. HANSEN, JANET RADWAY STONE, and JOHN W. LANE, JR.

Water-Resources Investigations Report 99-4050

Prepared in cooperation with the
U.S. ENVIRONMENTAL PROTECTION AGENCY, REGION 1

Northborough, Massachusetts
1999

U.S. DEPARTMENT OF THE INTERIOR
BRUCE BABBITT, Secretary

U.S. GEOLOGICAL SURVEY
Charles G. Groat, Director

The use of trade or product names in this report is for identification purposes only and does not constitute endorsement by the U.S. Geological Survey.

For additional information write to:

Chief, Massachusetts-Rhode Island District
U.S. Geological Survey
Water Resources Division
10 Bearfoot Rd.
Northborough, MA 01532

Copies of this report can be purchased from:

U.S. Geological Survey
Information Services
Box 25286
Denver, CO 80225-0286

CONTENTS

Abstract	1
Introduction	2
Description of Study Area	4
Acknowledgments	4
Geophysical-Survey Methods	8
Azimuthal Square-Array Resistivity	8
Acoustic Televiewer	8
Borehole Video	9
Single-Hole Directional Radar	9
Fracture Orientation and Relative Distribution Determined by Geophysical Methods	10
Azimuthal Square-Array Resistivity	10
Acoustic Televiewer	10
Single-Hole Directional Radar	16
Integrated Fracture Orientation	16
Correction of Fracture Density	18
Water-Yielding Fractures	20
Orientation and Distribution	20
Hydraulic Characteristics	25
Summary and Conclusions	25
References	26

FIGURES

1. Map showing locations of Eastern Surplus Superfund Site and the study area, Meddybemps, Maine	3
2. Map showing locations of geophysical survey sites and wells	5
3. Orientation and distribution of fractures measured on bedrock roadcuts along Route 191 in Meddybemps and Baring, Maine	7
4. Azimuthal plots of apparent resistivity and strike of high-angle fractures interpreted from square-array surveys at sites 1-3, Eastern Surplus Superfund Site	11
5. Orientation and distribution of all fractures observed on acoustic-televiewer logs from bedrock wells	12
6. Orientation and distribution of fractures observed on acoustic-televiewer logs of individual bedrock wells	13
7. Orientation and distribution of all fractures identified on single-hole directional radar records from bedrock wells	17
8. Orientation and probable density distribution of all fractures	19
9. Orientation and distribution of fractures that were detected only by single-hole directional radar surveys	20
10. Orientation and distribution of water-yielding fractures interpreted from televiewer and flowmeter logs of bedrock wells	21
11. Orientation and probable density distribution of water-yielding fractures	24

TABLES

1. Records of selected bedrock wells in and near the Eastern Surplus Superfund Site, Meddybemps, Maine..... 6

2. Summary of fracture type and orientation determined by four methods of observation 16

3. Orientation and estimated hydraulic properties of water-yielding fractures and fracture zones in bedrock wells, Eastern Surplus Superfund Site 22

CONVERSION FACTORS, VERTICAL DATUM, AND ABBREVIATIONS

CONVERSION FACTORS

Multiply	By	To obtain
foot (ft)	0.3048	meters
foot per nanosecond (ft/ns)	0.3048	meter per nanosecond
foot per second (ft/s)	0.0003	kilometer per second
foot squared per day (ft ² /d)	0.09290	meter squared per day
gallon (gal)	3.785	liter
gallons per minute (gal/min)	0.06308	liters per second
miles (mi)	1.609	kilometers

Temperature in degrees Fahrenheit (°F) can be converted to degrees Celsius (°C) as follows:
 $^{\circ}\text{C} = 5/9 (^{\circ}\text{F}-32)$.

VERTICAL DATUM

Sea level: In this report, "sea level" refers to the National Geodetic Vertical Datum of 1929 (NGVD of 1929)—a geodetic datum derived from a general adjustment of the first-order level nets of the United States and Canada, formerly called Sea Level Datum of 1929.

ABBREVIATIONS

MHz megahertz
 mho/m mho per meter
 µg/L micrograms per liter

Characteristics of Fractures in Crystalline Bedrock Determined by Surface and Borehole Geophysical Surveys, Eastern Surplus Superfund Site, Meddybemps, Maine

By Bruce P. Hansen, Janet Radway Stone, and John W. Lane, Jr.

Abstract

Surface and borehole geophysical methods were used to determine fracture orientation in crystalline bedrock at the Eastern Surplus Superfund Site in Meddybemps, Maine. Fracture-orientation information is needed to address concerns about the fate of contaminants in ground water at the site. Azimuthal square-array resistivity surveys were conducted at 3 locations at the site, borehole-acoustic televiewer and borehole-video logs were collected in 10 wells, and single-hole directional radar surveys were conducted in 9 wells. Borehole-video logs were used to supplement the results of other geophysical techniques and are not described in this report.

Analysis of azimuthal square-array resistivity data indicated that high-angle fracturing generally strikes northeast-southwest at the three locations. Borehole-acoustic televiewer logs detected one prominent low-angle and two prominent high-angle fracture sets. The low-angle fractures strike generally north-northeast and dip about 20 degrees west-northwest. One high-angle fracture set strikes north-northeast and dips east-southeast; the other high-angle set strikes east-northeast and dips south-southeast. Single-hole directional radar surveys identified two prominent fracture sets: a low-angle set striking north-northeast, dipping west-northwest; and a high-angle fracture set striking north-northeast, dipping east-southeast. Two additional high-angle fracture

sets are defined weakly, one striking east-west, dipping north; and a second striking east-west, dipping south.

Integrated results from all of the geophysical surveys indicate the presence of three primary fracture sets. A low-angle set strikes north-northeast and dips west-northwest. Two high-angle sets strike north-northeast and east-northeast and dip east-southeast and south-southeast. Statistical correction of the fracture data for orientation bias indicates that high-angle fractures are more numerous than observed in the data but are still less numerous than the low-angle fractures.

The orientation and distribution of water-yielding fractures sets were determined by correlating the fracture data from this study with previously collected borehole-flowmeter data. The water-yielding fractures are generally within the three prominent fracture sets observed for the total fracture population. The low-angle water-yielding fractures primarily strike north-northeast to west-northwest and dip west-northwest to south-southwest. Most of the high-angle water-yielding fractures strike either north-northeast or east-west and dip east-southeast or south. The spacing between water-yielding fractures varies but the probable average spacing is estimated to be 30 feet for low-angle fractures; 27 feet for the east-southeast dipping, high-angle fractures; and 43 feet for the south-southeast dipping, high-angle fractures.

The median estimated apparent transmissivity of individual water-yielding fractures or fracture zones was 0.3 feet squared per day and ranged from 0.01 to 382 feet squared per day. Ninety-five percent of the water-yielding fractures or fracture zones had an estimated apparent transmissivity of 19.5 feet squared per day or less.

The orientation, spacing, and hydraulic properties of water-yielding fractures identified during this study can be used to help estimate the recharge, flow, and discharge of ground water and contaminants. High-angle fractures provide vertical pathways for ground water to enter the bedrock, interconnections between low-angle fractures, and, subsequently, pathways for water flow within the bedrock along fracture planes. Low-angle fractures may allow horizontal ground-water flow in all directions. The orientation of fracturing and the hydraulic properties of each fracture set strongly affect changes in ground-water flow under stress (pumping) conditions.

INTRODUCTION

Recent sampling (1997) by the U.S. Environmental Protection Agency (USEPA) at the Eastern Surplus Superfund Site in Meddybemps, Maine (fig. 1) detected volatile organic compounds (VOCs) in ground water from surficial deposits and shallow bedrock in two areas (Roy F. Weston, Inc., written commun., 1997). VOCs in one of these areas can potentially flow through fractures in the bedrock to a hypothesized local cone of depression in the bedrock potentiometric surface centered east of the Dennys River (F.P. Lyford and others, U.S. Geological Survey, written commun., 1997). It is postulated that the cone of depression is caused by pumping from a domestic bedrock well. Shallow bedrock wells drilled in the study area in November 1996, ranging in depth from

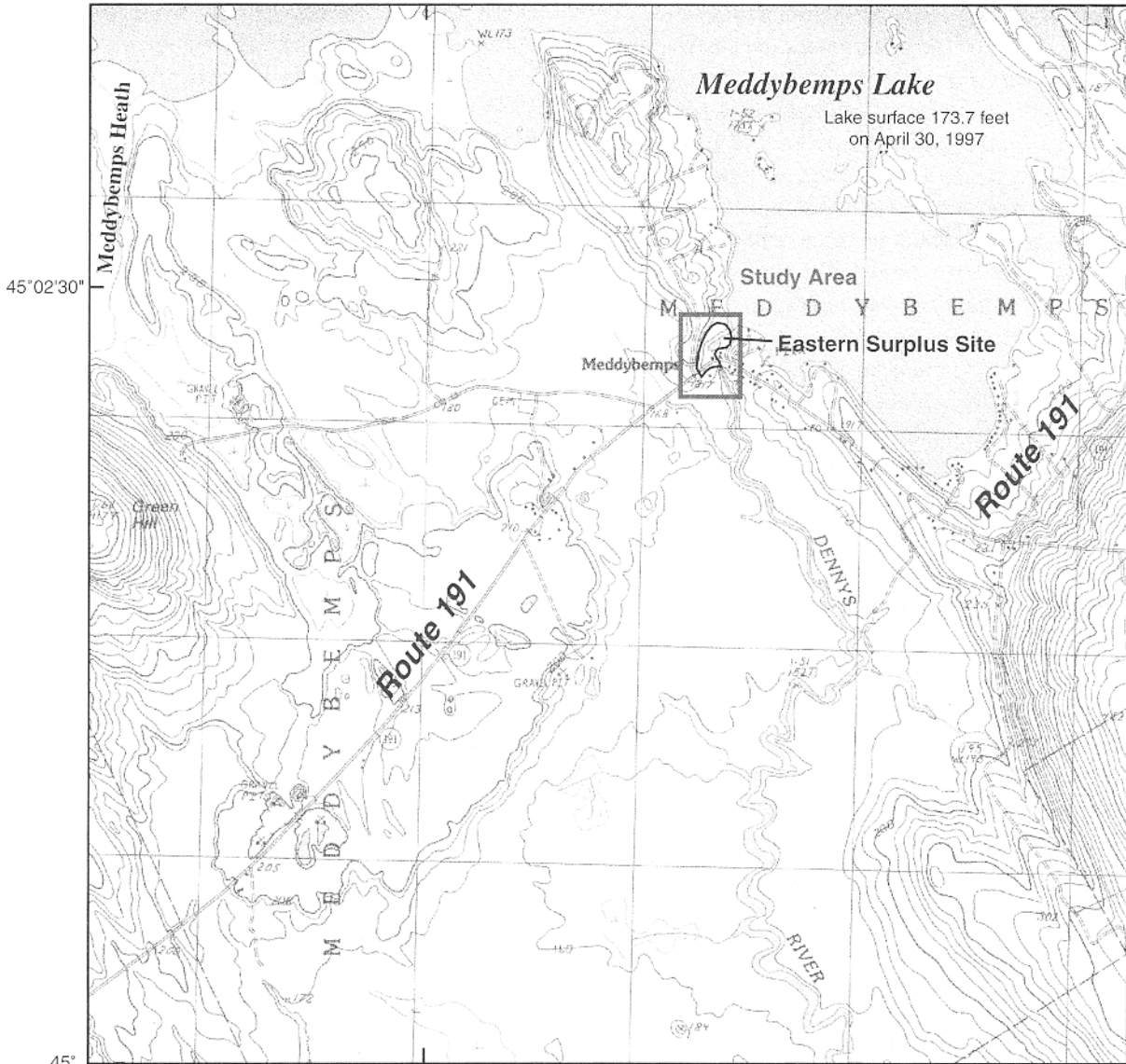
117 to 240 ft below land surface, intercepted water-yielding fractures. Information about fracture characteristics at the site is needed to determine the fate of contaminants in bedrock and to formulate ground-water remediation strategies.

During 1997 and 1998, the U.S. Geological Survey (USGS), in cooperation with the USEPA, studied bedrock fracture characteristics near the Eastern Surplus Superfund Site using several integrated methods, including geologic mapping, surface and borehole geophysics, and aquifer testing. This report describes bedrock fracture orientations and distributions near the Site that were determined by surface and borehole geophysical surveys, including azimuthal square-array resistivity, borehole video, borehole acoustic televiewer, and single-hole directional radar. An integrated interpretation of bedrock fracture orientations and distributions, based on all of the geophysical and geologic information available, is presented. Also described are the characteristics of water-yielding fractures, including orientation, distribution, probable average fracture spacing, and estimated hydraulic properties. Borehole-flowmeter data collected during an earlier study (Lyford and others, 1998) were used to identify water-yielding fractures and, in conjunction with the results of hydraulic testing of bedrock wells (F.P. Lyford and others, 1999), to estimate the hydraulic properties of fractures.

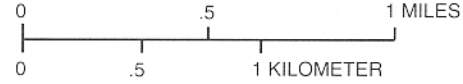
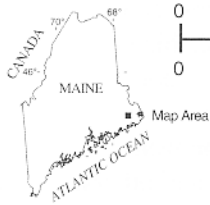
Most of the fracture data in this report are presented on rose diagrams and stereonet, two common techniques used to visually represent fracture data. The rose diagram is a specialized histogram used to represent the distribution of dip azimuth. The data are plotted in an angular fashion. The length of each angular segment is proportional to the number of fractures that have a dip azimuth within that particular segment. The stereonet displays a three-dimensional fracture orientation, showing not only dip azimuth but also dip angle. Equal-area, lower-hemisphere, polar-projection stereonet of data are presented in this report. For clarity, lines of longitude and latitude that normally appear on stereonet have been omitted.

67° 22' 30"

67° 20'



Base from U.S. Geological Survey
 Meddybemps Lake East and Meddybemps Lake West
 Quadrangles, 1:24,000, provisional edition 1987



TOPOGRAPHIC CONTOUR INTERVAL IS 10 FEET
 NATIONAL GEODETIC VERTICAL
 DATUM OF 1929

Figure 1. Locations of Eastern Surplus Superfund Site and the study area, Meddybemps, Maine.

Each point on the stereonet represents the intersection of the pole of a fracture-plane surface that passes through the center of the sphere with the surface of the lower hemisphere. The stereonet shows the intersection as if the surface of the lower hemisphere is viewed from the top of the upper hemisphere. For example, a cluster of points on the eastern edge of a stereonet would represent fractures that dip steeply to the west. Horizontal fractures would be represented by points near the center of the stereonet. On most of the stereonets shown in this report the density (relative abundance at any three-dimensional location) of plotted data in relation to a random distribution is shown. These density plots allow a visual determination of the central tendency of the strike and dip of fracture sets. On some of the stereonets, the actual data points have not been plotted.

Description of Study Area

The study area (fig. 1) is in northeastern Maine adjacent to Route 191 in the Town of Meddybemps and encompasses the Eastern Surplus Superfund Site. The background, hydrogeology, and water quality of the study area are described by Lyford and others (1998).

Two types of intrusive igneous bedrock underlie the region that encompasses the study area (Ludman, 1982; Osberg and others, 1985). Generally, the region is underlain by Meddybemps Granite; however, most of the study area is underlain, at least at shallow depth, by a small Gabbro-Diorite Intrusive Complex (Ludman and Hill, 1990). The presence of potassium feldspar in the granite and not in the gabbro-diorite make the two rock types easily distinguishable on borehole gamma logs. Although bedrock is not exposed within the study area, bedrock core, drill cuttings, and borehole gamma logs of nine wells installed during a previous study (Lyford and others, 1998) confirm that the upper 100–200 ft of bedrock is largely gabbro-diorite. Well MW-16B on the eastern edge of the study area (fig. 2; table 1) penetrated 40 ft of gabbro-diorite before penetrating 60 ft of granite, and well MW-14B on the northern edge of the area penetrated about 30 ft of granite at the bottom of the well. As indicated by Ludman and Hill (1990), this small area of gabbro-diorite is probably a detached body of mafic rock floating in the Meddybemps Granite.

The regional strike of bedrock fracturing, as seen in the grain of topography in bedrock hills on topographic maps and areal photographs, is NW-SE and ENE-WSW (nearly E-W) (Lyford and others, 1998). Fracture orientations were measured on the nearest outcrops to the study area along Route 191 east of Meddybemps Lake and on Green Hill to the west of the study area. Some of the outcrops along Route 191 were granite, and several were gabbro-diorite complex with cross-cutting granitic dikes. Green Hill is composed of granite. Two predominant high-angle fracture sets were measured with linear orientations (fig. 3) similar to those observed in the topography. One set strikes approximately NNW (N 25°–30° W) with a near vertical dip, and a second set strikes ranging from ENE to E (almost E-W) dipping steeply south. Several fractures on one outcrop had a strike of N 60° W. Generally, the NW-striking fractures were spaced 1–3 ft apart and the E-W-striking fractures were spaced 2–10 ft apart. Nearly horizontal fractures, spaced 1–6 ft apart, also were present.

In crystalline bedrock, ground water is present largely within fractures, only a few of which transmit measurable quantities of ground water. Borehole-flowmeter measurements were made in 25- to 193-foot sections of nine wells at the study site. Typically, only one to three water-yielding fractures or fracture zones were detected in each well with the borehole flowmeter. One exception was well MW-10B, where 16 water-yielding fracture or fracture zones were detected. The borehole flowmeter can detect changes in flow of approximately 0.02 gal/min. Yields estimated for the bedrock wells in the study area ranged from about 0.1 to 25 gal/min (table 1).

Acknowledgments

The authors thank Terry Lord, Greg Smith, Harry Smith, Madge Orchard, and Mona Van Wart for permission to conduct geophysical surveys on their property; and Edward Hathaway, Project Manager, U.S. Environmental Protection Agency, for facilitating access to survey locations. Appreciation also is extended to USGS employees Peter Joesten, for assisting with borehole radar surveys; Kevin Knutson, for doing borehole-televiewer and television surveys; Forest Lyford, for providing technical guidance and administrative assistance; William Nichols, for assisting with geophysical surveys; and Joseph Nielsen, for monitoring water levels.

EXPLANATION

DC-RESISTIVITY SQUARE-ARRAY
AZIMUTHAL SURVEYS—Number
is identification number

BEDROCK WELL WHERE BOREHOLE
RADAR, TELEVIEWER AND
TELEVISION SURVEYS
WERE CONDUCTED

WELL AND NUMBER

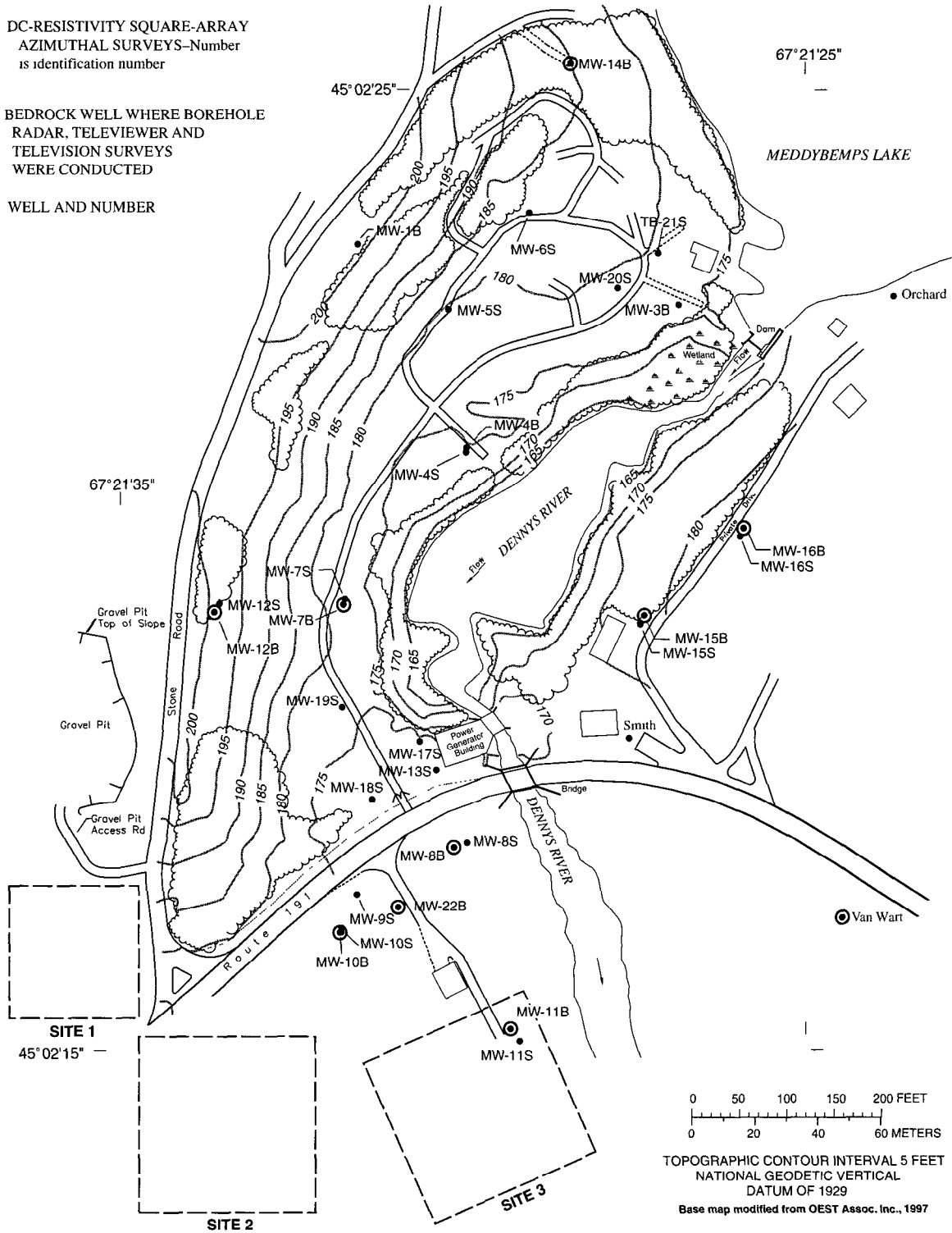
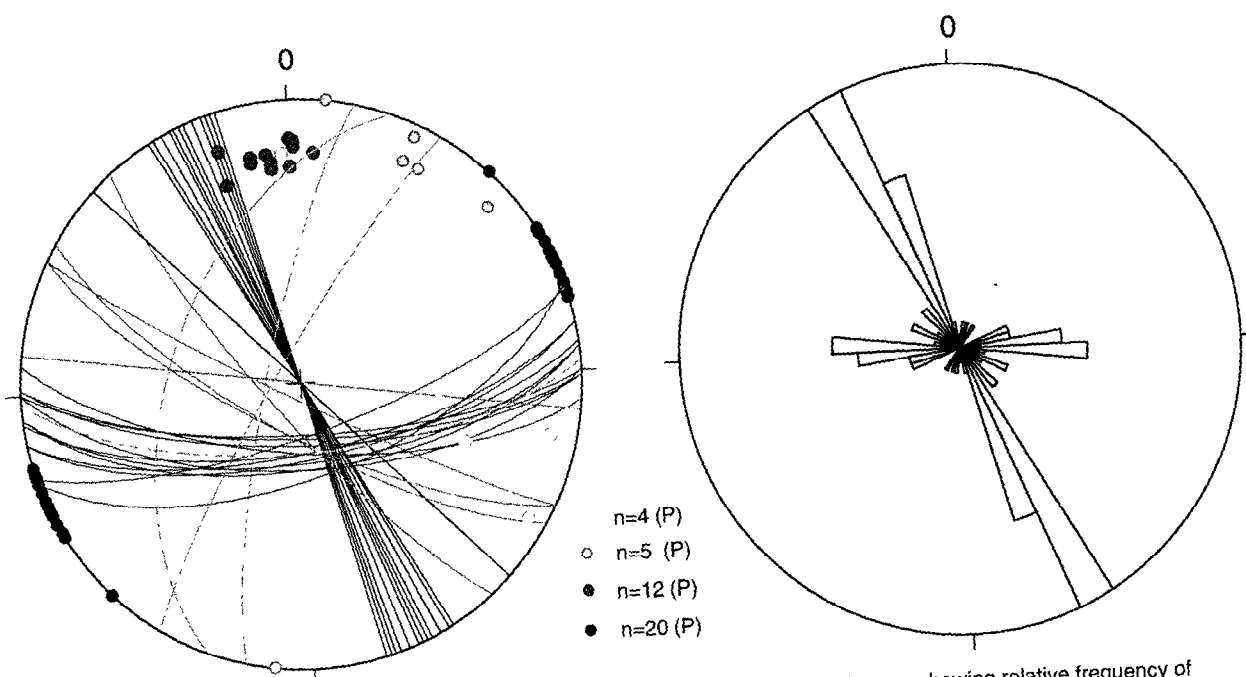


Figure 2. Locations of geophysical survey sites and wells, Eastern Surplus Superfund Site, Meddybemps, Maine.

Table 1. Records of selected bedrock wells in and near the Eastern Surplus Superfund site, Meddybemps, Maine

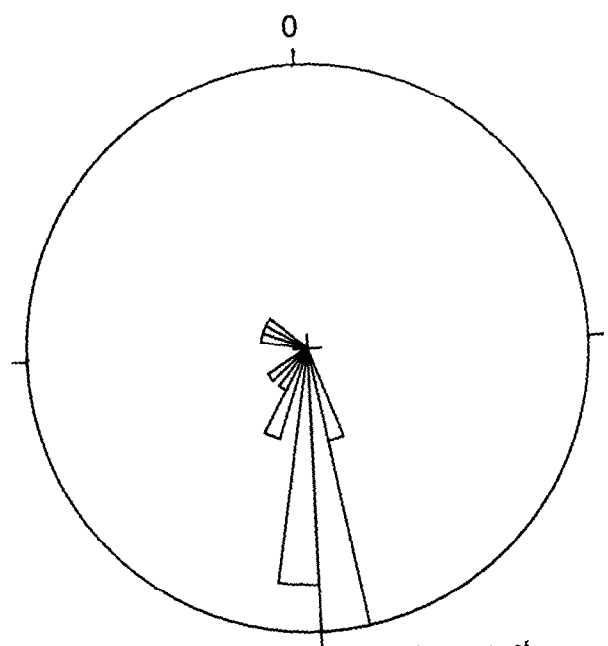
[All depths and open-hole intervals are in feet below land surface. **Altitude of land surface:** In feet above sea level. **Depth to water-yielding fracture zones:** Number in parentheses next to fracture zone indicates relative magnitude of yield while pumping, where (1) is the highest yielding fracture zone. **Remarks:** Pumping and drawdown measured by personnel of Roy F. Weston, Inc. (written commun., 1997) while sampling in December 1996. ft, foot; min, minute; gal/min, gallon per minute; --, no data; >, actual value is greater than value shown; <, actual value is less than value shown]

Well No. or name	Date drilled	Altitude of land surface	Total depth of borehole	Depth to bedrock	Altitude of bedrock surface	Open-hole interval	Approximate yield (gal/min)	Depth to water-yielding fracture zones	Remarks
MW-7B	10-28-96	177.81	117.8	18	159.8	21-117.8	>0.004	89	No measurable flow in borehole for static condition. No flow measurements above depth of 48.6 ft during pumping because of drawdown.
MW-8B	11-04-96	169.04	124	20.5	148.5	25.7-124	.06	27-34 (2) 55-65 (1)	No measurable flow in borehole for static conditions.
MW-10B	11-04-96	174.24	120	20	154.2	26.4-120	1.2	30-31 (1) 72-76 (2) 37 (3)	Drawdown of 1.6 ft after 161 min while pumping at 0.07 gal/min. Static flow is downward from fractures from 26 to 60 ft to fractures from 60 to 85 ft. Water-yielding fractures also observed at 33-35, 41-42, 55, 63-66, 80-83, 94-96, 101-107, and 110 ft.
MW-11B	11-04-96	169.69	132	29	140.7	34-132	15	34-41 (2) 71-74 (3) 77-80 (1)	Drawdown of 1.4 ft after 90 min while pumping at 0.42 gal/min. No measurable flow in borehole for static conditions. Water-yielding fractures also at 88 and from 128 to 130 ft.
MW-12B	11-04-96	200.13	138	22.5	177.6	27.7-138	.03	34-37	No measurable flow in borehole for static conditions.
MW-14B	11-05-96	185.70	120	3.5	182.2	9.4-120	.5	25-27	Drawdown of 1.45 ft after 105 min while pumping at 0.21 gal/min. No measurable flow in borehole for static conditions. No flow measurements above 24 ft during pumping because of drawdown.
MW-15B	11-05-96	178.97	240	39	140.0	46.9-240	.06	73-78 (1) 92-95 (1)	No measurable flow in borehole for static conditions. Flow from two zones approximately equal.
MW-16B	11-05-96	182.18	140	38	144.2	42.3-140	.09	45-46 (1) 68-68.5 (3) 108-118 (2)	No measurable flow in borehole for static conditions.
MW-22B	1950s	172.35	49	18	154.4	25-49	25	25.5-30	Former residential well. Yield reported by former owner (E. Gillespie, oral commun., 1996). No measurable flow in borehole for static conditions.
Van Wart	--	171.78	142	29	142.8	39-142	5	--	Residential well. Yield reported by driller (T. Lord, oral commun., 1996).
Smith	--	173.35	420	--	--	--	<.3	--	Residential well. Yield reported by driller (T. Lord, oral commun., 1996)



Lower-hemisphere, equal-area stereonet plot of poles to fracture planes and trace of fracture intersections with lower-hemisphere. Total number of fractures plotted is 41.

Rose diagram showing relative frequency of measured fracture strike, in 15° classes.



Rose diagram showing relative frequency of measured fracture dip direction, in 2° classes.

Fracture orientation measurements made on low-relief bedrock roadcuts that are oriented NNW to NNE.

Figure 3. Orientation and distribution of fractures measured on bedrock roadcuts along Route 191 east of the study site in Meddybemps and Baring, Maine.

GEOPHYSICAL-SURVEY METHODS

The geophysical methods applied in this study were azimuthal square-array resistivity, borehole acoustic televiewer, borehole video, and single-hole directional radar. Integration (cross-correlation) of the results from various independent surveys improved confidence in the orientation and location of fractures and also improved resolution (degree to which individual features can be detected) over that of a single method. Individual surveys were made in as close proximity to one another as practically possible, so that the same or approximately similar volumes of bedrock were sampled. The methods used for this study were selected because of their successful use for fracture detection and characterization in previous investigations at other sites in New Hampshire, Massachusetts, and New Jersey (Lieblich and others, 1991, 1992a, and 1992b; Hansen and Lane, 1995; Paillet and Ollila, 1994; Morin and others, 1997).

Azimuthal Square-Array Resistivity

Azimuthal square-array resistivity was used to measure directional variations in apparent earth resistivity. These variations are related to sets of similarly oriented, steeply dipping fractures. The theory, development, and application of this method as it was used in this study is described in Lane and others (1995) and Hansen and Lane (1995).

The square array consists of four electrodes driven into the ground to form a square configuration. The location of all measurements are assigned to the center point of the square. The array size (A) is the length of a side of the square. Each resistivity measurement consists of measuring current (I) between two current electrodes (A and B) and the potential difference between two potential electrodes (M and N). On the basis of these measurements, apparent resistivity is determined using equations presented in Hansen and Lane (1995, p. 6). For each square, three apparent resistivity measurements are taken. Two measurements (alpha and beta) are perpendicular to each other and parallel to the sides of the square, and a third (gamma) is diagonal across the square. The two perpendicular measurements provide information on the directional variations of the subsurface resistivity. The azimuthal orientation of the perpendicular

measurements is the line that connects the current electrodes. The diagonal measurement serves as a check on the accuracy of the two perpendicular measurements. In an isotropic medium, the apparent resistivity in the alpha and beta directions are equal and gamma is equal to zero. In a homogeneous, anisotropic medium, the gamma resistivity is equal to the difference between the alpha and beta resistivity. To collect a complete set of azimuthal-profiling data, the array is rotated in equal angular increments around a common center point. To detect vertical (depth) variations in apparent resistivity at each azimuthal orientation, the array is usually expanded symmetrically about the center point. These resistivity soundings can be interpreted as a function of depth. Each array samples a cube of earth with dimensions approximately equal to the array A -spacing.

Fracture strike can be determined graphically or analytically. To graphically interpret fracture strike at a site, each apparent resistivity for a given size square and the azimuth of that measurement are plotted. The principal fracture strike direction is perpendicular to the direction of maximum resistivity. Fracture strike can be determined analytically based on resistivity data from two squares separated by 45° (crossed square array) and applying equations presented by Habberjam (1972; 1975).

Acoustic Televiewer

The borehole acoustic televiewer (hereafter referred to as "televiewer") provides a photograph-like image representing the pattern of acoustic reflectivity on the borehole wall. The image is orientated with respect to the Earth's magnetic field. The irregular surface where a fracture intersects a borehole usually appears as an elliptical line on the televiewer record. The shape and vertical extent of this ellipse can be used to determine apparent fracture strike and dip with respect to the borehole axis. In cases where the borehole is deviated from the vertical, true strike and dip can be determined if borehole deviation is known (Kierstein, 1983; Lau, 1983). The televiewer-logging system used for this investigation collected data on acoustic velocity and amplitude, magnetic orientation, and deviation. All of the data were stored in digital format. The data were interpreted using interactive computer processing that produced a compilation of

the true strike and dip of observed fractures, orientated hole-diameter logs, and orientated cross-sectional and plan-view plots of borehole deviation. All fracture orientations were corrected for borehole deviation. All magnetic north azimuths were adjusted to true north. Televiewer instrumentation and interpretation are described in more detail by Keys (1990) and Zemanek and others (1969).

Ten wells at the Eastern Surplus Site were logged with the televiewer. One well (MW-7B) was too small in diameter (2.75 in.) for proper operation of the televiewer, so the record from this well was unusable.

Borehole Video

Borehole video logs were collected for the purpose of visually inspecting the cased and uncased sections of bedrock wells. Video logs were collected by a vertically oriented color video camera that provided a 360-degree image of the borehole wall. A light mounted below the camera illuminated several feet of borehole wall below the camera. The camera was normally focused on the most brightly illuminated section of borehole wall, and the depth encoder was set to record the depth of this point. A video monitor with an onscreen depth display was used to view the optical image of the borehole as the camera was lowered into the subsurface. A permanent record of the video was produced by simultaneously recording the video data onto tape, which could be used for later review of borehole conditions. The horizontal azimuthal orientation of the video camera was unknown and, therefore, fracture strike could not be determined from the video record. A description of a borehole video logging system is given by Safko and Hickey (1992).

The clarity of the video images was directly related to the transparency of the water in the borehole at the time of each survey. In general, the quality of the record from most of the 10 wells surveyed was good. However, because of other logging activities that created turbid water, the record from well MW-11B was very poor and the records from wells MW-22B and MW-8B were fair.

The video records were used mainly in conjunction with televiewer logs to clarify fracture geometry, particularly in fracture zones where fractures

with different overlapping orientations intersected the borehole. Video records also were used to examine the bottom of the casing for evidence of water leakage. The video surveys are not presented in this report.

Single-Hole Directional Radar

Single-hole directional radar surveys were done to detect the location and orientation of fractures or fracture zones. These surveys were done with an MALA GeoScience RAMAC borehole-radar system. A broad-band electric-dipole transmitting antenna with a center frequency of 60 MHz was used with a directional-receiving antenna consisting of four separate loop antennas oriented orthogonally. Directional information about a reflection is obtained by measuring the phase difference of the incoming wave on the different antenna elements. The frequency used was selected to provide an acceptable compromise between high resolution (the degree to which individual features can be detected) and deep penetration (the distance that the radar wave travels into rock). For this study, the transmitter and directional receiver were lowered into the same well with the antenna center points separated by 27.9 ft. Incremental stacked measurements were made every 0.82 ft along the length of each well. Data were processed and interpreted with MALA software. The analysis software allows the interpretation of the strike, dip, and projected borehole-intersection depth of planar discontinuities. The distance and direction to pointlike discontinuities also can be interpreted.

The velocity of radar waves through the rock adjacent to the borehole was determined by collecting a vertical radar profile (VRP). For this technique, either the transmitting or receiving antenna remains fixed in the borehole and the other antenna is moved away at 0.82 ft increments. Total traveltime of the direct wave between the transmitting and receiving antenna at each station is measured. The traveltime data are used with the known distance between the antennas to calculate the direct-wave radar velocity through each increment of borehole. Theory, development, and previous use of borehole-radar systems is summarized in references cited by Lane and others (1994) and Hansen and Lane (1995).

FRACTURE ORIENTATION AND RELATIVE DISTRIBUTION DETERMINED BY GEOPHYSICAL METHODS

Graphic displays of data from azimuthal square-array resistivity, borehole-acoustic televiewer, and single-hole borehole-radar surveys are presented in this section. Fracture orientations determined with these methods and from examination of bedrock outcrops are summarized.

Azimuthal Square-Array Resistivity

Azimuthal square-array data collected at three sites (fig. 2) indicated variations in apparent resistivity with measurement direction. At each site, these variations changed as the size of the array increased. At small array spacings, resistivity anomalies (resistivity highs with corresponding orthogonal resistivity lows) were small and randomly distributed. These small and random anomalies probably resulted from heterogeneities in the unconsolidated surficial deposits that were investigated (sampled) at small array spacings. Resistivity data from large array spacings, which sample a large volume of bedrock, were used to interpret the large-scale orientation of high-angle fractures. Azimuthal plots of resistivity data for sites 1–3 (fig. 2) at array spacings of 148, 212, and 148 ft, respectively, are shown in figure 4. Resistivity data for an array spacing of 42 ft for site 3 also is shown in figure 4. Data from other array spacings were used for analysis but are not shown. The graphical plots of resistivity data indicate the following:

- At site 1, the primary high-angle fracture strike orientation is generally NNE and probably ranges from N to ENE.

- At site 2, the primary high-angle fracture strike orientation is generally NE and ranges from NNE to ENE.
- At site 3, at shallow bedrock depths (less than 42 ft), the primary high-angle fracture strike orientation is generally NE and generally E at greater depths.

Acoustic Televiewer

Fracture orientation and relative distribution of all fractures observed on televiewer logs from nine wells (fig. 2) are shown in figure 5. Three fracture sets are indicated by the relative distribution of the data on the lower-hemisphere stereonet data plots. A low-angle fracture set (less than 45° dip) generally strikes NNE and dips WNW. The strike of individual fractures in this low-angle set range slightly more than 90° E and W of the centralized strike. This low-angle fracture set has an average dip of 18° but varies from 0 to 45°. Two high-angle fracture sets are indicated by the data plots. In general, these sets strike NNE and ENE and dip ESE and SSE, respectively.

Fracture orientation and density in each of the nine wells logged with the televiewer are shown in figure 6. In general, fracture populations within individual wells correspond to one or more of the three generalized fracture sets shown by the data for all fractures in figure 5 but vary from well to well. A few wells have fracture sets that do not correspond to the generalized fracture sets described above. The absence of observed very high-angle or vertical fractures in any of the wells is probably the result of a very high negative sampling bias because the wells are vertical.

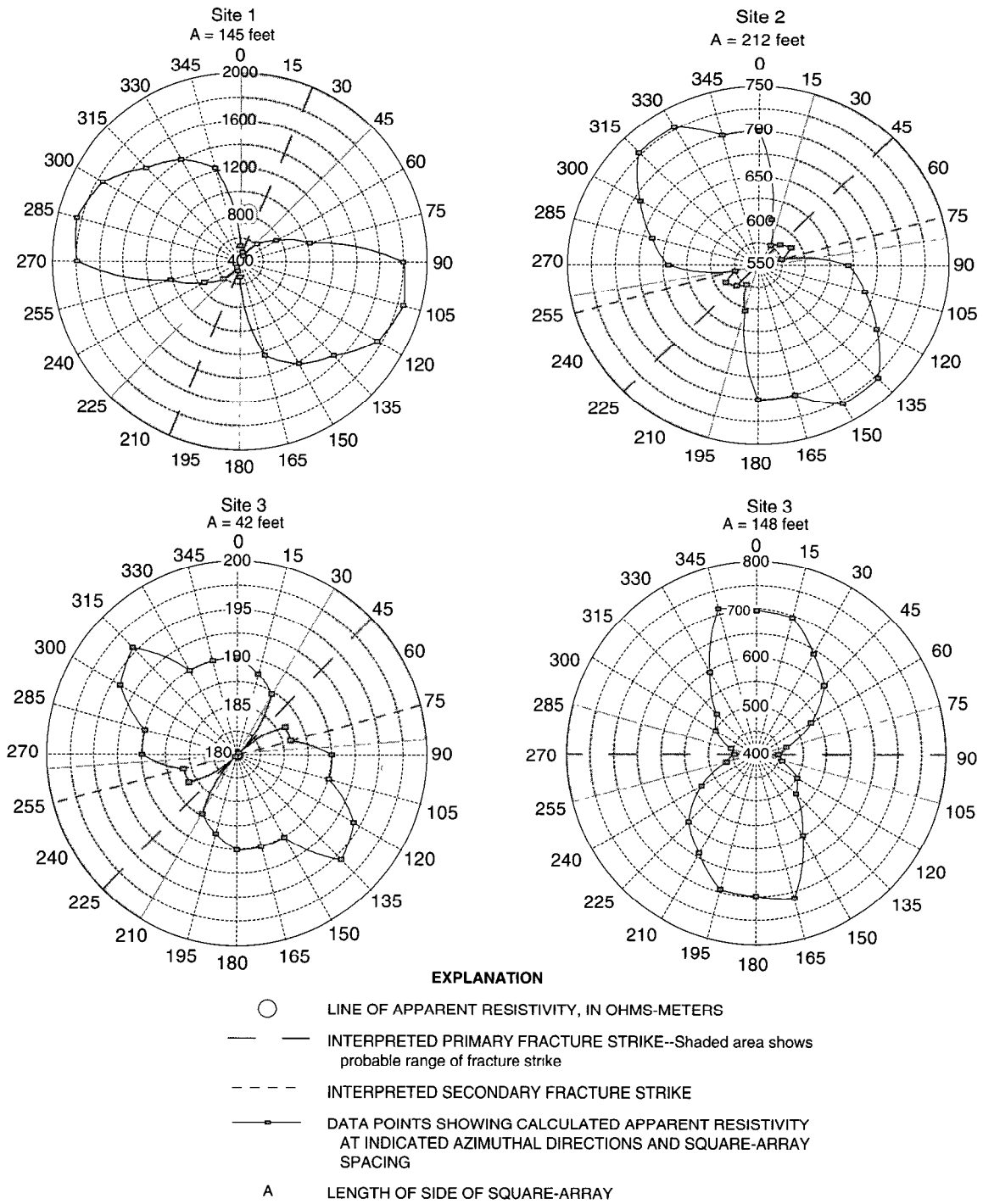
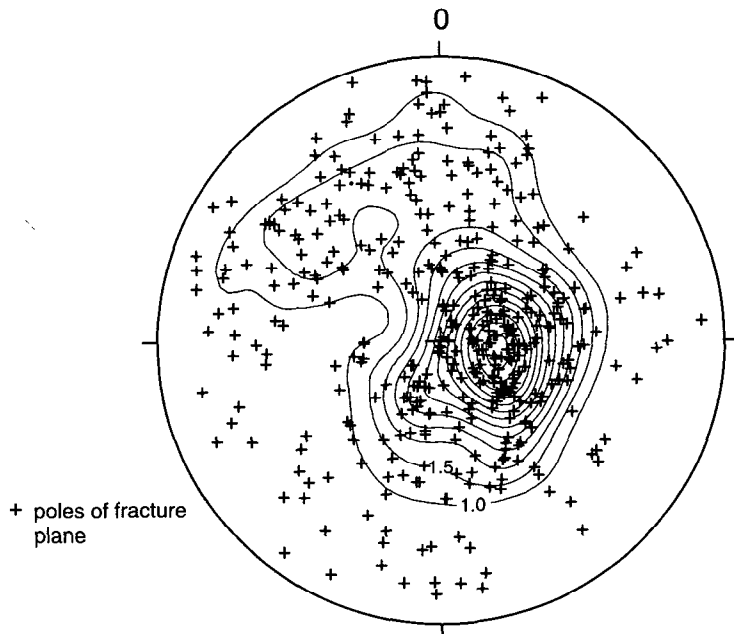
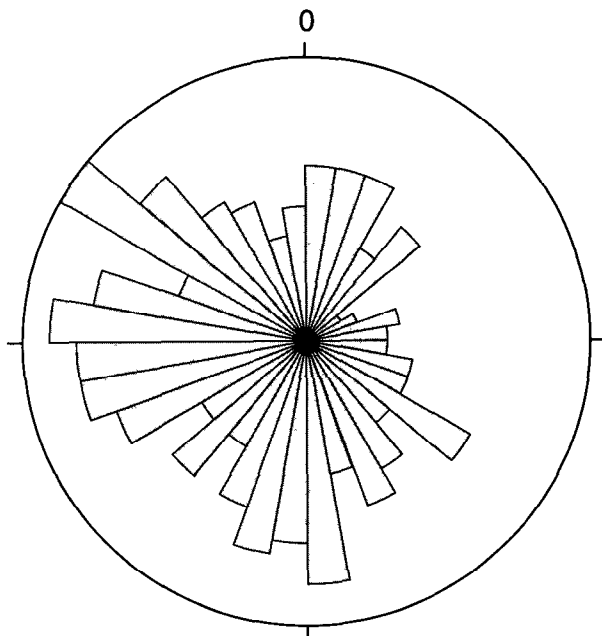


Figure 4. Azimuthal plots of apparent resistivity and strike of high-angle fractures interpreted from square-array surveys at sites 1–3, Eastern Surplus Superfund Site, Meddybemps, Maine.



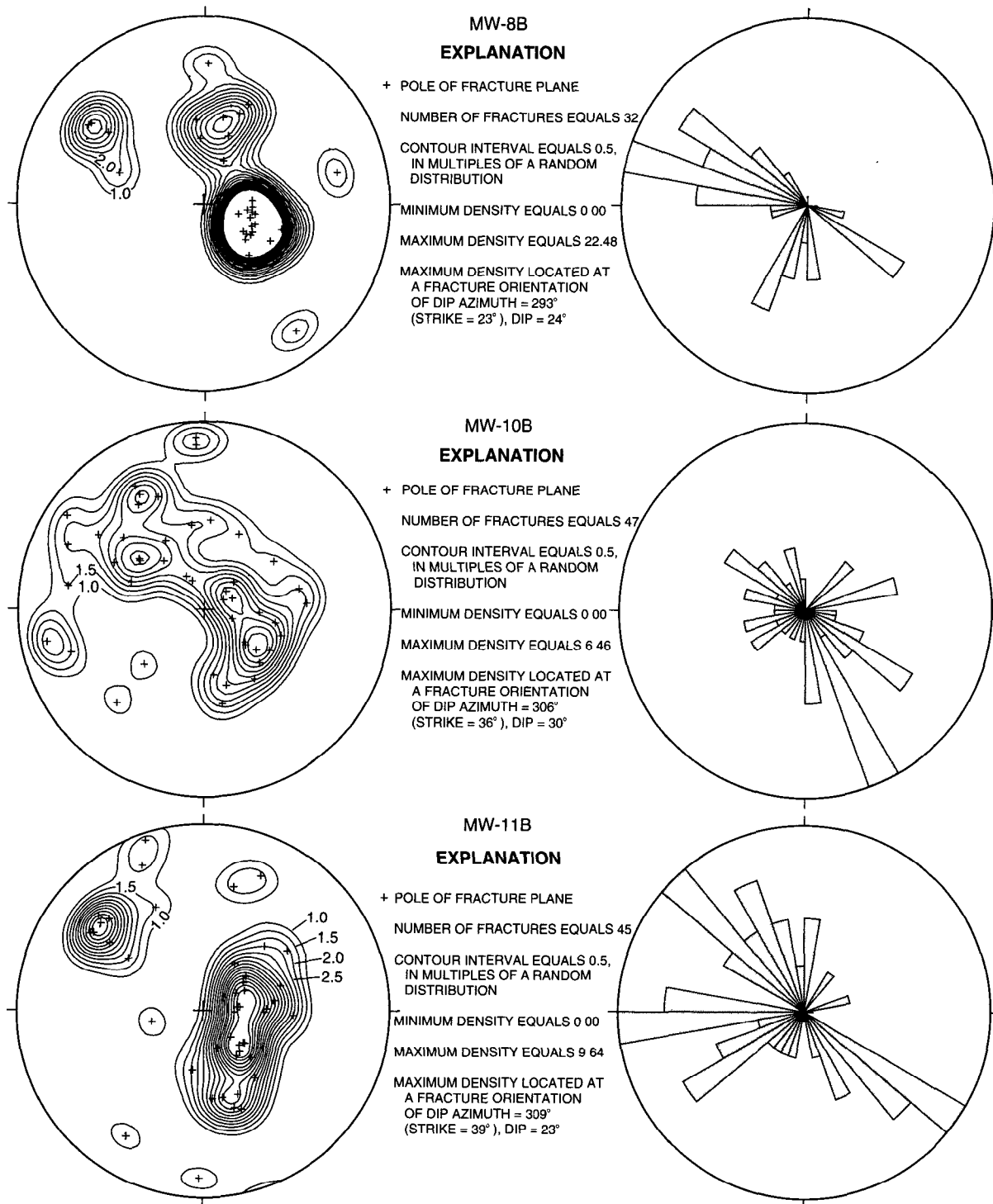
Lower-hemisphere, equal-area stereonet plot of poles to fracture planes and contour plot of relative orientation distribution density of fractures.

EXPLANATION
 CONTOUR INTERVAL EQUALS 0.5, IN MULTIPLES OF A RANDOM DISTRIBUTION
 NUMBER OF FRACTURES EQUALS 421
 MINIMUM DENSITY EQUALS 0.00
 MAXIMUM DENSITY EQUALS 7.24
 MAXIMUM DENSITY LOCATED AT A FRACTURE ORIENTATION OF DIP AZIMUTH = 276° (STRIKE = 186°), DIP = 15°



Rose diagram showing frequency of observed fracture dip direction, in 10° classes.

Figure 5. Orientation and distribution of all fractures observed on acoustic-televiwer logs from bedrock wells, Eastern Surplus Superfund Site, Meddybemps, Maine.



Lower-hemisphere, equal-area stereonet plots of poles to fracture planes and contour plot of relative orientation distribution density of fractures.

Rose diagrams showing probable frequency of fracture dip direction, in 10° classes.

Figure 6. Orientation and distribution of all fractures observed on acoustic-televiwer logs of individual bedrock wells, Eastern Surplus Superfund Site, Meddybemps, Maine.

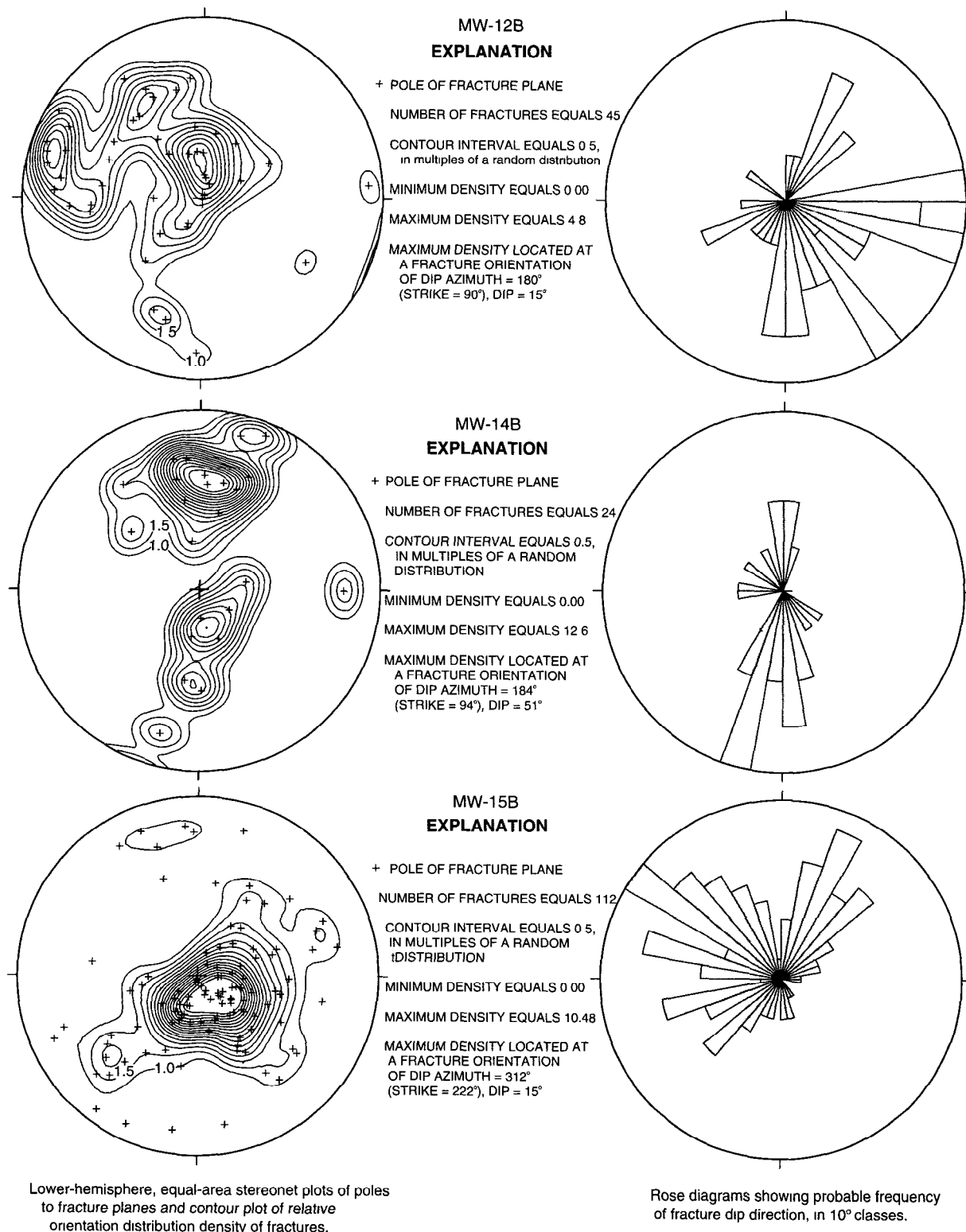
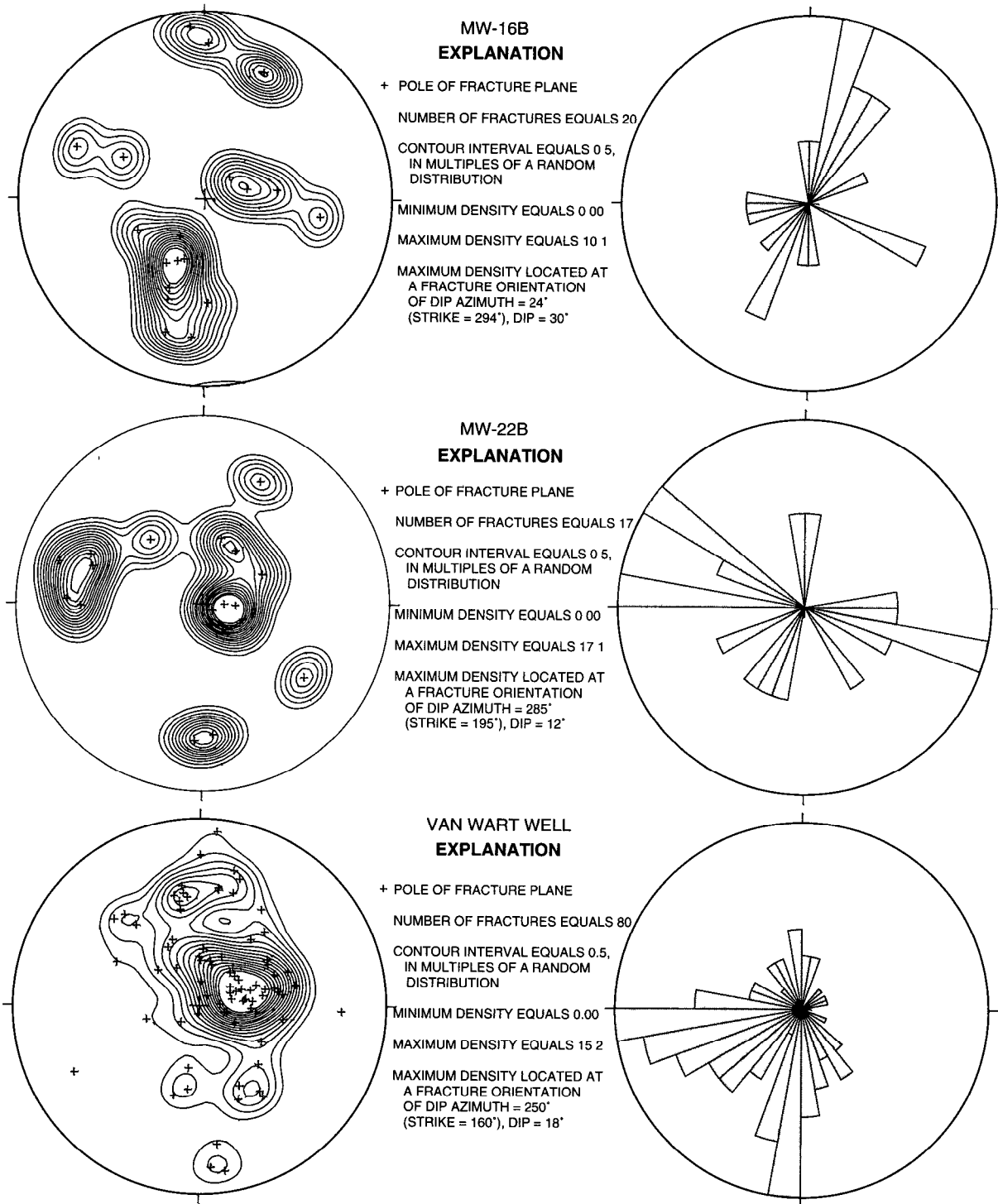


Figure 6. Orientation and distribution of all fractures observed on acoustic-televiewer logs of individual bedrock wells, Eastern Surplus Superfund Site, Meddybemps, Maine—*Continued.*



Lower-hemisphere, equal-area stereonet plots of poles to fracture planes and contour plot of relative orientation distribution density of fractures.

Rose diagrams showing probable frequency of fracture dip direction, in 10° classes.

Figure 6. Orientation and distribution of all fractures observed on acoustic-televiwer logs of individual bedrock wells, Eastern Surplus Superfund Site, Meddybemps, Maine—*Continued.*

Single-Hole Directional Radar

The radar records from eight wells (no usable data from the Van Wart well) indicate that radar-wave penetration into the bedrock averaged about 25 ft and ranged from 0 to 50 ft. Radar velocity ranged from 0.26 to 0.32 ft/ns. Calculated dielectric permittivity (Beres and Haeni, 1991) of the crystalline rock ranged from 9.4 to 14.2, which is higher than typically reported for a wet granite (Ulriksen, 1982; Markt, 1988) and indicates relatively conductive materials. The calculated resolution of the radar record (the degree to which individual fractures can be detected) averages about 2.4 ft (Sheriff, 1984; Trabant, 1984). Applying the average radar-wave velocity and data from the radar records, the location and orientation of each radar reflector (fracture or fracture zone) was determined. A total of 224 fractures were identified. The orientation and distribution of fracture density for all the fractures identified from the single-hole directional radar records is shown in figure 7. The data indicate a predominant set of low-angle fractures with an average NNE strike (WNW dip azimuth) that ranges from NE counterclockwise to NW (dip azimuths range from NW to SW). The low-angle fracture set has an average dip of about 18°. A high-angle fracture set striking

NNE and dipping ESE is clearly indicated, and two high-angle sets striking E-W and dipping N and S, respectively, are weakly indicated.

Integrated Fracture Orientation

An integrated interpretation of all of the data from the various survey methods indicates the presence of three fracture sets:

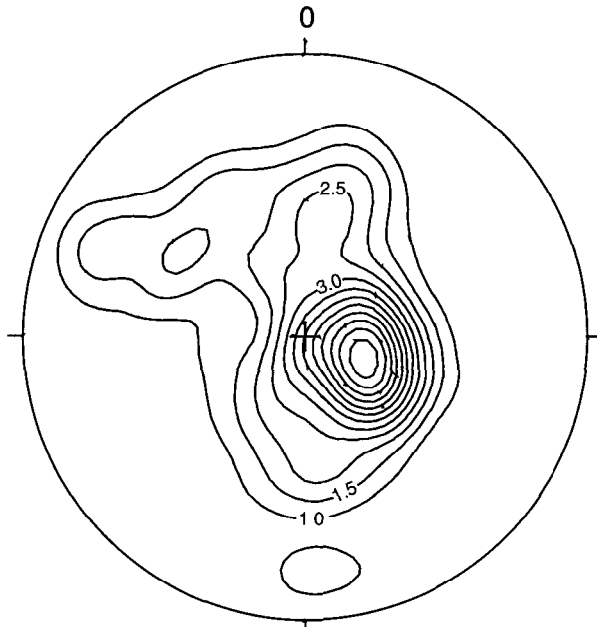
- a low-angle set striking NNE and dipping WNW;
- a high-angle set striking NNE and dipping ESE; and
- a second high-angle set striking ENE to E (nearly EW) and dipping SSE to S.

The NNE-striking low-angle fractures were observed on televiewer and directional radar logs. Within this low-angle fracture set there is considerable variation in strike and dip azimuth (figs. 5 and 6). Both of the high-angle fracture sets were indicated by outcrop mapping, square-array resistivity, and televiewer surveys. The NNE-striking high-angle fractures are either vertical (outcrop data) or high angle (televiewer and directional radar data). The vertical NNW-striking fracture set observed on outcrops is weakly indicated by some of the square-array results and is not listed as a major fracture set. A summary of the fracture sets determined by the various surveying methods is listed in table 2.

Table 2. Summary of fracture type and orientation determined by four methods of observation, Meddybemps, Maine

[Azimuths relative to True North; °, degrees; Low-angle fractures, dip equals from 0 to 45 degrees; High-angle fractures, dip equals 45 to 90 degrees]

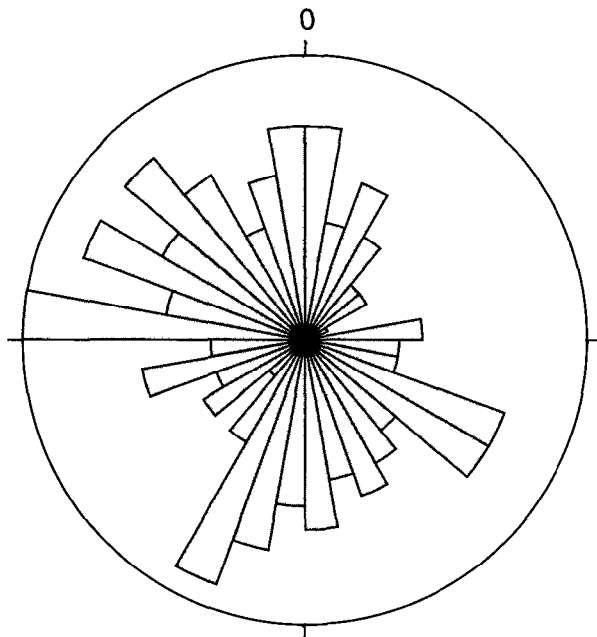
Method of observation	Fracture type and orientation			
	High-angle fractures		Low-angle fractures	
	Strike	Dip and dip azimuth	Strike	Dip and dip azimuth
Outcrop Mapping	NNW	90° (vertical)	Horizontal and very low-angle fractures observed. Orientation not measured.	
	ENE to E-WSW to W	75-80° SSE to S		
Square-Array Resistivity	NNE-SSW	Not detected by this method	Not detected by this method	
	NE-SW			
	NE-SW			
	E-W			
Acoustic Televiewer	NNE-SSW	75° ESE	NNE-SSW	18° WNW
	ENE-WSW	75° SSE		
Directional Radar	NNE-SSW	60° ESE	NNE-SSW	18° WNW
	E-W	70° N		
	E-W	70° S		



Lower-hemisphere, equal-area stereonet plot of poles to fracture planes and contour plot of relative orientation distribution density of fractures.

EXPLANATION

NUMBER OF FRACTURES EQUALS 224
 CONTOUR INTERVAL EQUALS 0.5,
 IN MULTIPLES OF A RANDOM DISTRIBUTION
 MINIMUM DENSITY EQUALS 0.00
 MAXIMUM DENSITY EQUALS 6.91
 MAXIMUM DENSITY LOCATED AT
 A FRACTURE ORIENTATION
 OF DIP AZIMUTH = 290°
 (STRIKE = 208°), DIP = 18°



Rose diagram showing probable frequency of fracture dip direction, in 10° classes.

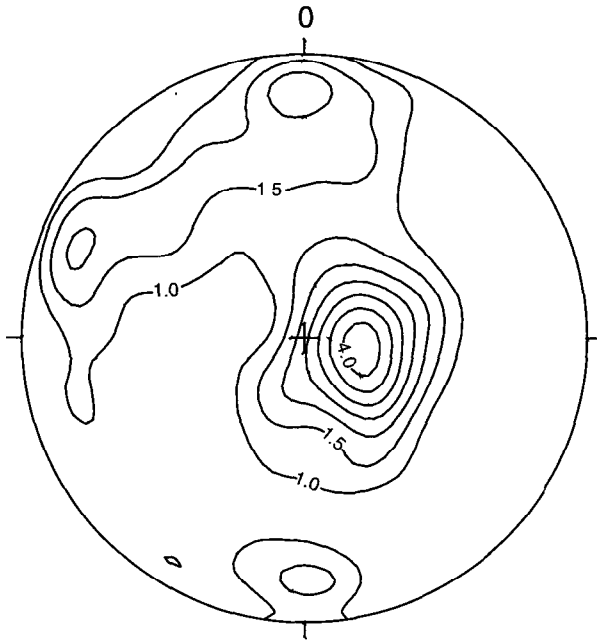
Figure 7. Orientation and distribution of all fractures identified on single-hole directional radar records from bedrock wells, Eastern Surplus Superfund Site, Meddybemps, Maine.

CORRECTION OF FRACTURE DENSITY

The relative abundance of observed fractures with different orientations is partially related to biases associated with the orientation of the field observations. Examination of fractures on horizontal or low-relief outcrops has a higher probability of detecting vertical and high-angle fractures than detecting horizontal fractures. Conversely, vertical boreholes have a high probability of intersecting horizontal fractures and almost zero probability of intersecting a vertical fracture. To account for this sampling bias, a correction based on the orientation of the scan line used to sample fracture orientation (90° for vertical boreholes), and the dip angle of the observed fracture may be applied to a fracture population to determine the probable density (numbers) of fractures actually present. The probable abundance of fractures in a set would be equivalent to the number of fractures intersected by a well drilled normal to their planes. The number of fractures in any equal-area segment (an area bounded by a small range of strike and dip) is multiplied by the inverse of the cosine of the dip angle (Terzaghi, 1965) to determine the probable number of fractures present at the indicated strike

and dip. This method has been used in several recent fracture studies (Barton and Zoback, 1992; Morin and others, 1997).

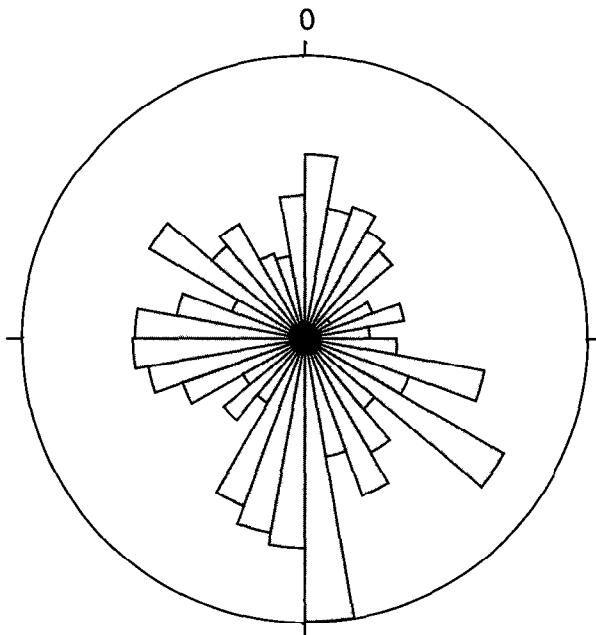
A probability correction was done with the cumulative televiewer fracture-population data from nine wells. The resulting lower-hemisphere equal-area contour plot of fracture density and rose diagrams of fracture dip azimuth are shown in figure 8. The three primary fracture sets are still defined, but the corrected plot indicates that steeply dipping fractures are probably significantly more numerous than observed in boreholes (fig. 5). A larger population of high-angle fractures than was observed on the televiewer record is supported by the radar data, which indicate more high-angle fractures (reflectors) than the televiewer records. The radar logs sampled a much larger horizontal distance than the televiewer (0.5 ft for the televiewer and an average of 50 ft for the radar) in each well. Fractures that were detected by the directional radar but not detected by the televiewer are shown in figure 9. The fractures shown on this figure either do not intersect the surveyed wells or intersect the planes of the wells above or below the open sections of the wells.



Lower-hemisphere, equal-area stereonet contour plot of probable relative orientation distribution density of fractures.

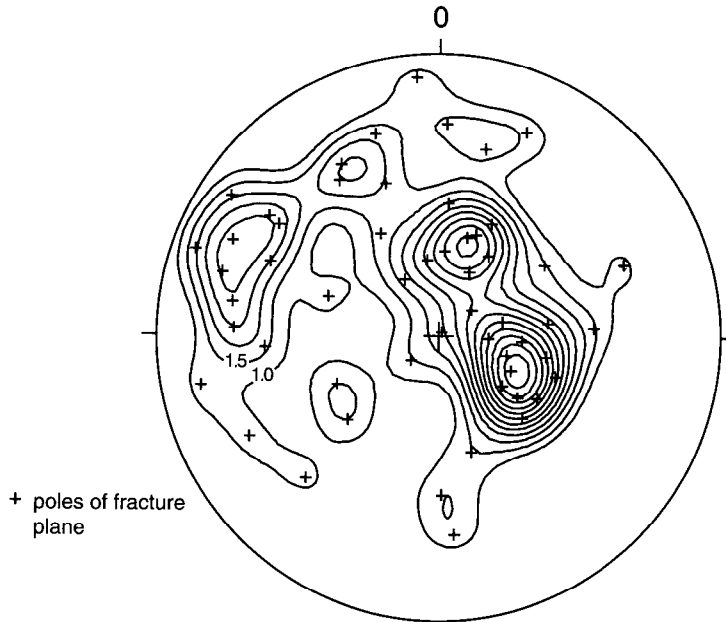
EXPLANATION

NUMBER OF FRACTURES EQUALS 421
 CONTOUR INTERVAL EQUALS 0.5,
 IN MULTIPLES OF A RANDOM DISTRIBUTION
 MINIMUM DENSITY EQUALS 0.00
 MAXIMUM DENSITY EQUALS 4.3
 MAXIMUM DENSITY LOCATED AT
 A FRACTURE ORIENTATION
 OF DIP AZIMUTH = 280°
 (STRIKE = 190°), DIP = 18°



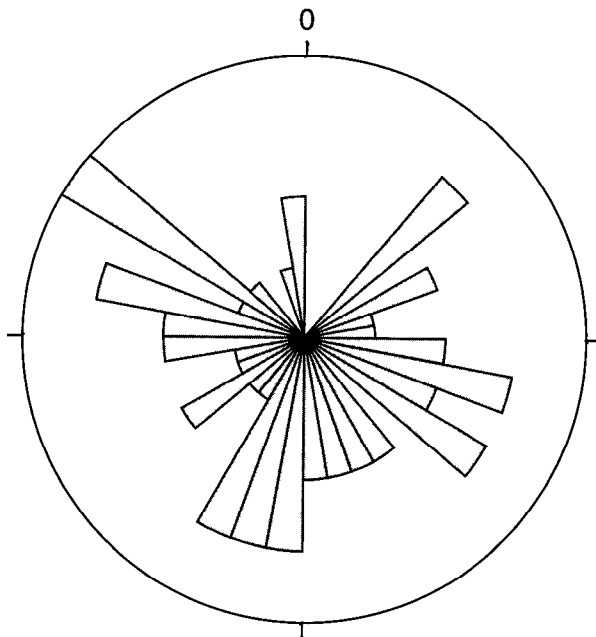
Rose diagram showing probable frequency of fracture dip direction, in 10° classes.

Figure 8. Orientation and probable density distribution of all fractures, Eastern Surplus Superfund Site, Meddybemps, Maine.



Lower-hemisphere, equal-area stereonet plot of poles to fracture planes and contour plot of relative orientation distribution density of fractures.

EXPLANATION
 NUMBER OF FRACTURES EQUALS 56
 CONTOUR INTERVAL EQUALS 0.5,
 IN MULTIPLES OF A RANDOM DISTRIBUTION
 MINIMUM DENSITY EQUALS 0.00
 MAXIMUM DENSITY EQUALS 6.9
 MAXIMUM DENSITY LOCATED AT
 A FRACTURE ORIENTATION
 OF DIP AZIMUTH = 293°
 (STRIKE = 203°), DIP = 66°



Rose diagram showing probable frequency of fracture dip direction, in 10° classes.

Figure 10. Orientation and distribution of water-yielding fractures interpreted from televiwer and flowmeter logs of bedrock wells, Eastern Surplus Superfund Site, Meddybemps, Maine.

Table 3. Orientation and estimated hydraulic properties of water-yielding fractures in bedrock wells, Eastern Surplus Superfund site, Meddybemps, Maine

[All depths in feet below indicated datum. Azimuth in degrees relative to true north. Shaded areas indicate intersecting fractures or fracture zones. Total estimated apparent transmissivity for each well is average from Lyford and others, U.S. Geological Survey, written commun., 1998. No, number; ft, foot; ft²/d, foot squared per day; --, no data; >, actual value is greater than value shown; <, actual value is less than value shown; *, probable yielding fracture in fracture zone or where fractures intersect]

Well No. or name	Depth below top of casing	Depth below land surface	Strike azimuth (degrees)	Dip azimuth (degrees)	Dip (degrees)	Estimated apparent transmissivity (ft ² /d)	Remarks
MW-8B	31.5–32.5	31.2–32.2	92.0	182.0	63.9		
	31.9–32.1	31.6–31.8	205.3	295.3	23.1	0.07	
	58.7–58.9	58.4–58.6	115.1	205.1	20.4		
	59.4–59.7	59.1–59.4	109.9	199.9	31.3	.11	
	76.9–78.0	76.6–77.7	35.0	125.0	62.5	.02	
Well total						0.2	
MW-10B	28.0–28.5	26.6–27.1	--	--	38.4		
	28.0–28.9	26.6–27.5	--	--	59.6	2.14	
	33.7–34.0	32.3–32.6	224.5	314.5	34.4	3.98	
	35.1–35.4	33.7–34.0	211.5	301.5	33.7	.18	
	36.2–36.4	34.8–35.0	218.9	308.9	22.7	.52	
	39.6–40.1	38.2–38.7	177.1	267.1	45.7	.15	
	45.9–46.3	44.5–44.9	253.9	343.9	34.7	.52	
	52.0–53.5	50.6–52.1	24.7	114.7	69.4		
	54.5–56.9	53.1–55.5	33.3	123.3	76.6		
	57.5–57.1	56.1–55.7	215.5	305.5	28.5	.52	
	63.1–63.4	51.7–62.0	190.9	280.9	31.9	.31	
	64.8–65.2	63.4–63.8	199.0	289.0	35.7		
	68.1–68.5	66.7–67.1	146.1	236.1	37.0		
	68.2–69.0	66.8–67.6	313.1	43.1	58.0	.43	
	70.7–71.5	69.3–70.1	57.2	147.2	54.0	.12	
	74.5–75.5	73.1–74.1	34.6	124.6	58.3		
	76.5–77.6	75.1–76.2	9.1	99.1	63.2		
	78.4–78.8	77.0–77.4	115.3	205.3	36.3	1.77	
	79.1–79.5	77.7–78.1	19.3	109.3	34.2		
	81.5–81.9	80.1–80.5	317.3	47.3	36.2	.09	
83.2–83.5	81.8–82.1	60.0	150.0	34.2	.30		
96.2–96.4	94.8–95.0	184.4	274.4	23.9			
97.0–99.2	95.6–97.8	348.6	78.6	74.8	.06		
104.3–104.4	102.9–103.0	141.7	231.7	12.4	.09		
112.7–113.1	111.3–111.7	94.0	184.0	38.7			
113.0–113.9	111.6–112.5	60.2	150.2	58.5	.30		
Well total						11.5	

Table 3. Orientation and estimated hydraulic properties of water-yielding fractures in bedrock wells, Eastern Surplus Superfund site, Meddybemps, Maine—*Continued*

Well No. or name	Depth below top of casing	Depth below land surface	Strike azimuth (degrees)	Dip azimuth (degrees)	Dip (degrees)	Estimated apparent transmissivity (ft ² /d)	Remarks
MW-11B	36.0–40.0	35.1–39.1	--	--	--	16.2	fracture orientation unknown
	75.5–76.2	74.6–75.3	103.7	193.7	57.5	5.4	
	79.4–80.6	78.5–79.7	113.0	193.7	57.5	64.8	
	130.0–130.2	129.1–129.3	218.1	308.1	23.3	3.6	
Well total						90	
MW-12B	33.2–33.7	32.0–32.5	355.9	85.9	51.7	.16	
	36.3–36.3	35.1–35.1	131.3	221.3	1.2		
	*36.7–40.0	35.5–38.8	19.4	109.4	80.7	.14	
Well total						0.3	
MW-14B	16.0–16.5	14.4–14.9	268.5	358.5	46.7	19.5	
	28.8–29.0	27.2–27.4	81.1	171.1	22.2	6.5	
Well total						26	
MW-15B	77.1–77.3	76.0–76.2	196.4	286.4	20.3	.04	
	*94.7–95.7	93.6–94.6	158.9	248.9	59.6		
	95.9–97.0	94.8–95.9	72.2	162.2	63.8		
	97.6–98.2	96.5–97.1	70.3	160.3	47.7	.06	
Well total						0.1	
MW-16B	48.8–49.1	47.1–47.4	173.1	263.1	32.0	.14	
	68.7–69.0	67.0–67.3	334.3	64.3	32.7		
	69.2–69.4	67.5–67.7	167.5	257.5	18.8	.01	
	100.4–103.8	98.7–102.1	84.9	174.9	80.0	.05	
Well total						0.2	
MW-22B	30.6–31.3	28.7–29.4	23.6	113.6	54.9		
	31.5–32.8	29.6–30.9	16.2	106.2	68.8	382	
	35.9–36.2	34.0–34.3	121.8	211.8	27.1	6.5	
	37.0–37.3	35.1–35.4	105.7	195.7	29.6	8.3	
	43.7–43.8	41.8–41.9	183.5	273.5	14.4		
	43.4–44.2	41.5–42.3	265.1	355.1	59.4		
	44.2–45.2	42.3–43.3	1.9	91.9	61.7	16.5	
	>46.5	>44.6				1.7	
Well total						415	
Van Wart	91.8–91.9	90.4–90.5	318.1	48.1	10.6	5.33	
	94.4–94.6	93.0–93.2	58.5	148.5	18.9		
	95.0–96.1	93.6–94.7	331.9	61.9	64.8	6.40	
	97.7–97.9	96.3–96.5	93.6	183.6	24.6	.26	
Well total						12.0	



Lower-hemisphere, equal-area stereonet contour plot of probable relative orientation distribution density of fractures.

EXPLANATION

NUMBER OF FRACTURES EQUALS 56

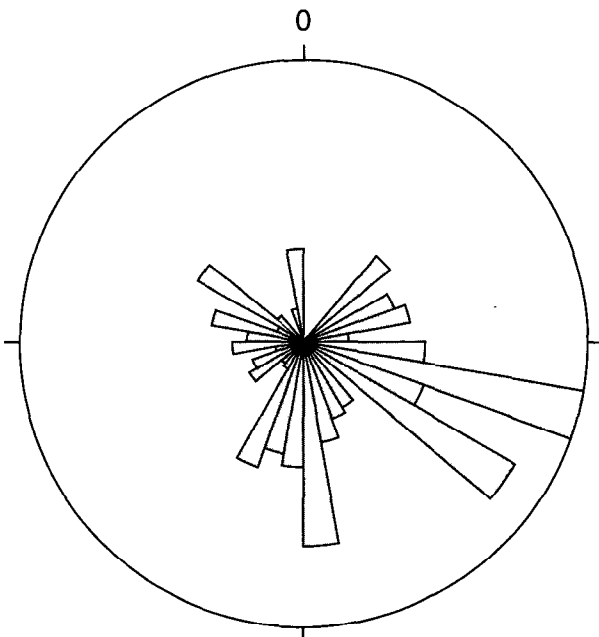
CONTOUR INTERVAL EQUALS 0.5,
IN MULTIPLES OF A RANDOM DISTRIBUTION

DENSITY CALCULATED USING A WEIGHTING
FACTOR OF $1/\text{COS OF DIP}$

MINIMUM DENSITY EQUALS 0.00

MAXIMUM DENSITY EQUALS 5.8

MAXIMUM DENSITY LOCATED AT
A FRACTURE ORIENTATION
OF DIP AZIMUTH = 113°
(STRIKE = 23°), DIP = 75°



Rose diagram showing probable frequency of fracture dip direction, in 10° classes.

Figure 11. Orientation and probably density distribution of water-yielding fractures, Eastern Surplus Superfund Site, Meddybemps, Maine.

On the basis of the data and a correction applied to account for sampling-orientation bias, the spacing and orientation of water-yielding fractures believed to be present at the Eastern Surplus area were estimated. Statistically, the average spacing (normal to the fracture planes) is estimated to be 30 ft for the low-angle fractures; 27 ft for the NNE-striking, ESE-dipping, high-angle fractures; and 43 ft for the ENE-striking, SSE-dipping high-angle fractures. However, the observed spacing of observed fractures is nonuniform. Some miscellaneous water-yielding high-angle fractures that are not in the main fracture groups are present and probably have an average spacing of 60 ft.

Hydraulic Characteristics

Flowmeter data, which provided the percentage of total well yield produced from each water-yielding fracture or fracture zone during the flowmeter testing, was combined with total apparent fracture transmissivity of each well determined by hydraulic testing (F.P. Lyford and others, U.S. Geological Survey, written commun., 1998) to estimate the apparent transmissivity of each fracture or fracture zone. The estimated transmissivities are listed in table 3. Median apparent transmissivity of individual fractures or fracture zones was 0.3 ft²/d. Apparent fracture transmissivity ranged from 0.01 to 382 ft²/d, but 95 percent of the fractures or fracture zones had an apparent transmissivity of 19.5 ft²/d or less. The largest apparent fracture transmissivity (382 ft²/d) was associated with a shallow high-angle fracture zone in well MW-22B. Aquifer-test results (F.P. Lyford and others, 1999) indicate that this zone may be hydraulically connected to coarse-grained unconsolidated material that overlies bedrock at this location. The largest apparent fracture transmissivity associated with a single fracture (58 ft²/d) is in well MW-11B (fig. 2). The hydraulic properties of this high-angle fracture and its location and orientation relative to wells MW-10B and MW-11B, which are separated by more than 200 ft, are probably the reason for the

good hydraulic connection observed between these two wells during aquifer testing (F.P. Lyford and others, 1999).

SUMMARY AND CONCLUSIONS

In 1997–98 the USGS, in cooperation with the USEPA, used four geophysical methods to determine fracture orientation in the crystalline bedrock that underlies the Eastern Surplus Superfund Site and adjacent areas in Meddybemps, Maine. The fracture information can be used to assess ground-water and contaminant transport at the site. Azimuthal square-array resistivity surveys were done at 3 sites, borehole-acoustic televiewer and borehole-video logs were collected in 10 wells, and single-hole directional radar surveys in 9 wells.

Azimuthal square-array resistivity data from three sites indicated that the primary high-angle fractures have a generally NE strike. At site 3, the data for depths greater than 42 ft indicated that the high-angle fracture strike shifted to east.

Borehole televiewer data from nine wells indicate the presence of three primary fracture sets, one low-angle set (< 45° dip) and two high-angle sets (> 45° dip). The low-angle fractures strike generally NNE and dip 20° to the WNW. The two high-angle fracture sets strike generally NNE and ENE and dip ESE and SSE, respectively. Observed fracture orientation and density differ considerably from well to well, but the three fracture sets were observed in most data plots from individual wells.

Single-hole directional radar data indicate two primary fracture sets: a low-angle fracture set striking NNE and dipping WNW, and a high-angle fracture set striking NNE and dipping ESE. Two additional high-angle fracture sets are defined weakly, one striking E-W and dipping N; and a second striking E-W and dipping S.

Integrated results from square-array resistivity, televiewer, single-hole directional radar surveys, and previous outcrop mapping indicate the presence of

three primary fracture sets. A low-angle fracture set strikes NNE and dips WNW. Two high-angle fracture sets strike NNE and ENE and dip ESE and SSE.

The total number of fractures with different orientations observed with methods used in this study are biased because of the orientation of the field observations. Fracture-population data were adjusted to determine the probable number of fractures present at the site. The corrected data indicate that the high-angle fractures are probably much more numerous than observed in the boreholes.

The orientation and distribution of water-yielding fracture sets were identified by combining the fracture data from this study with the results of borehole-flowmeter logging from a previous study. In general, water-yielding fracture sets correspond to the same three fracture sets as were observed for the total fracture population. In contrast to the total fracture population, most of the water-yielding fractures dip southerly. Most of the low-angle fractures strike generally from NNE to WNW and dip WNW to SSW. The probable average spacing (normal to the fracture plane) between water-yielding fractures in the three fracture sets is estimated to be 30 ft for the low-angle fractures; 27 ft for the NNE-striking, ESE-dipping high-angle fractures; and 43 ft for the ENE-striking and SSE-dipping high-angle fractures. Spacing between water-yielding fractures and fracture sets is variable.

The median estimated apparent transmissivity of individual fractures or fracture zones intersecting bedrock wells in the study area was 0.3 ft²/d and ranged from 0.01 to 382 ft²/d: 95 percent of the fractures or fracture zones had an apparent transmissivity of 19.5 ft²/d or less. The largest apparent transmissivity associated with a single fracture (58 ft²/d) is in well MW-11B. This high-angle fracture is probably responsible for the good hydraulic connection observed between well MW-11B and well MW-10B during aquifer testing.

The orientation, spacing, and hydraulic properties of water-yielding bedrock fractures identified by this study can be used to help determine recharge, flow, and discharge of ground water and contaminants. High-angle fractures provide vertical pathways for ground water to enter the bedrock, interconnections between low-angle fractures, and, subsequently, pathways for flow within the bedrock along fracture planes. Low-angle fractures may allow horizontal ground-water flow in all directions. The orientation of fracturing and the hydraulic properties of each fracture set will strongly affect changes in ground-water flow under stress (pumping) conditions.

REFERENCES

- Barton, C.A., and Zoback, M.D., 1992, Self-similar distribution and properties of macroscopic fractures at depth in crystalline rock in the Cajon Pass Scientific Drill Hole: *Journal of Geophysical Research*, v. 97, p. 5181–5200.
- Beres, Milan, Jr., and Haeni, F.P., 1991, Application of ground-penetrating-radar methods in hydrologic studies: *Ground Water*, v. 29, no. 3, p. 375–386.
- Haberjam, G.M., 1972, The effect of anisotropy on square array resistivity measurements: *Geophysical Prospecting*, v. 20, p. 249–266.
- 1975, Apparent resistivity, anisotropy and strike measurements: *Geophysical Prospecting*, v. 23, p. 211–247.
- Hansen, B.P. and Lane, J.W., Jr., 1995, Use of surface and borehole geophysical surveys to determine fracture orientation and other site characteristics in crystalline bedrock terrain, Millville and Uxbridge, Massachusetts: U.S. Geological Survey Water-Resources Investigations Report 95-4121, 25 p.
- Keys, W.S., 1990, Borehole geophysics applied to ground-water investigations: U.S. Geological Survey *Techniques of Water-Resources Investigations*, book 2, chap. E2, 150 p.
- Kierstein, R.A., 1983, True location and orientation of fractures logged with the acoustic televiewer: U.S. Geological Survey Water-Resources Investigations Report 83-4275, 71 p.

- Lane, J.W., Jr., Haeni, F.P., and Watson, W.M., 1995, Use of square-array direct-current resistivity method to detect fractures in crystalline bedrock in New Hampshire: *Ground Water*, v. 33, no. 3, p. 476–485.
- Lane, J.W., Jr., Haeni, F.P., and Williams, J.H., 1994, Detection of bedrock fractures and lithologic changes using borehole radar at selected sites, *in* Fifth International Conference on Ground-Penetrating Radar, Kitchener, Ontario, Canada, June 12–16, 1993, Proceedings: Waterloo, Ont., Can., Waterloo Centre for Groundwater Research, p. 577–591.
- Lau, J.S.O., 1983, The determination of true orientation of fractures in rock cores: *Canadian Geotechnical Journal*, v. 20, no. 3, p. 221–227.
- Lieblisch, D.A., Haeni, F.P., and Cromwell, R.E., 1992a, Integrated use of surface-geophysical methods to indicate subsurface fractures at Tibbetts Road, Barrington, New Hampshire: U.S. Geological Survey Water-Resources Investigations Report 92-4012, 33 p.
- Lieblisch, D.A., Lane, J.W., Jr., and Haeni, F.P., 1991, Results of integrated surface-geophysical studies for shallow subsurface fracture detection at three New Hampshire sites, *in* Expanded Abstracts with Biographies, SEG 61st Annual International Meeting, Houston, Texas, November 10–14, 1991: Houston, Tex., Society of Exploration Geophysicists, p. 553–556.
- Lieblisch, D.A., Haeni, F.P., and Lane, J.W., Jr., 1992b, Integrated use of surface-geophysical methods to indicate subsurface fractures at Milford, New Hampshire: U.S. Geological Survey Water-Resources Investigations Report 92-4056, 38 p.
- Ludman, Allan, 1982, Bedrock geology of the Fredericton 2-degree quadrangle, Maine: Maine Geological Survey, Open-File No. 82-30, 16 p., scale 1:250,000.
- Ludman, Allan, and Hill, Malcolm, 1990, Bedrock geology of the Calais 15' quadrangle, eastern Maine: Maine Geological Survey Open-File No. 90-27, 32 p., scale 1:62,500.
- Lyford, F.P., Garabedian, S.P., and Hansen, B.P., 1999, Estimated hydraulic properties for the surficial- and bedrock-aquifer system, Meddybemps, Maine: U.S. Geological Survey Open-File Report 99-199, ___ p.
- Lyford, F.P., Stone J.R., Nielsen, J.P., and Hansen, B.P., 1998, Geohydrology and ground-water quality, Eastern Surplus Superfund Site, Meddybemps, Maine: U.S. Geological Survey Water-Resources Investigations Report 98-4174, 68 p.
- Markt, George, 1988, Subsurface characterization of hazardous waste sites using ground-penetrating radar, *in* Second International Symposium on Geotechnical Applications of Ground-Penetrating Radar, March 6–10, 1988, Proceedings: 41 p.
- Morin, R.H., Carleton, G.B., and Poirier, Stephane, 1997, Fractured-aquifer hydrology from geophysical logs; the Passaic Formation, New Jersey: *Ground Water*, v. 35, no. 2, p. 328–338.
- Osberg, P.H., Hussey, A.M., and Boone, G.M. (eds.), 1985, Bedrock geologic map of Maine: Maine Geological Survey, scale 1:500,000.
- Paillet, F.L., and Ollila, Paul, 1994, Identification, characterization, and analysis of hydraulically conductive fractures in granitic basement rocks, Millville, Massachusetts: U.S. Geological Survey Water-Resources Investigations Report 94-4185, 36 p.
- Safko, P.S., and Hickey, J.J., 1992, A preliminary approach to the use of borehole data, including television surveys, for characterizing secondary porosity of carbonate rocks in the Floridan aquifer system: U.S. Geological Survey Water-Resources Investigations Report 91-4168, 70 p.
- Sheriff, R.E. 1984, Encyclopedic dictionary of exploration geophysics (2d ed.): Tulsa, Okla., Society of Exploration Geophysics, 323 p.
- Terzaghi, R.D., 1965, Sources of error in joint surveys: *Geotechnique*, v. 15, p. 287–304.
- Trabant, P.K., 1984, Applied high-resolution geophysical methods: Boston, International Human Resources Development Corp., 265 p.
- Ulriksen, P.F., 1982, Application of impulse radar to civil engineering: Lund, Sweden, Lund University of Technology, Ph.D. Thesis, 179 p.
- Zemanek, Joseph, Caldwell, R.L., Glen, E.E., Halcomb, S.V., Norton, L.J., and Strauss, A.J.D., 1969, The borehole televiewer—a new logging concept for fracture location and other types of borehole inspection: *Journal of Petroleum Technology*, v. 21, no. 6, p. 762–774.